Method for Mechanical Design of Squirrel Cage Slitted Solid Rotor

Juuso Narsakka, Konstantin Vostrov, Tuhin Choudhury, Emil Kurvinen, Jussi Sopanen, *Member, IEEE* and Juha Pyrhönen, *Senior Member, IEEE*

***Abstract*—The design of high-speed machines requires extensive multidisciplinary approach to achieve a high-performance machine. The design process is highly iterative, and analytical methods can accelerate it with faster design iterations at low computational efficiency to find the optimum parameters at conceptual stage. In this study, an analytical design method for obtaining rotor mechanical limits is developed for squirrel-cage slitted high-speed induction machine rotors. In high-speed electric machines, the design is made specifically to meet the application requirements and the objective is to reach a high efficiency. This means that the design needs to be made often from the scratch and existing designs can rarely be used as a starting point. The method developed in this study enables rapid design iterations, especially considering the mechanical limits in the conceptual and layout design phase. The proposed analytical design method is validated with three different case studies.**

***Index Terms*—Design space, High-speed machines, Squirrel cage, Slitted rotor, Induction motor, Rapid design**

I. Introduction

When designing a high-speed electrical machine one could say that the limiting factors, in the order of importance, come from rotor mechanical strength, rotor dynamic performance, heat transfer and finally the electromagnetic performance of the machine. Because of a need to achieve a high-strength and rigid rotor design often a solid rotor core is considered. The same approach is valid for both permanent-magnet and induction motors. A solid rotor core ensures a strong and rigid enough rotor construction. In addition, it usually can offer acceptable rotordynamic properties. [1], [2] The trend for building higher power, high-speed machines creates design challenges in manufacturing high-strength and highly rigid rotors. Producing more output power is challenging due to the limiting factors, e.g. stress and rotordynamics which makes the physical size increase challenging, i.e the solution scalability is poor. In case of an induction motor, a smooth solid rotor is the simplest solution but, however, not a favourable option as the machine properties with a smooth rotor are poor. Therefore, a solid rotor needs improvements to guarantee acceptable performance. The minimum improvement is reached by slitting the rotor surface with axial slits. This forces the magnetic flux penetrate much deeper in the rotor than in case of a smooth rotor. Slitting also increases the high-frequency surface impedance and, thus, helps in minimising rotor surface losses. Manufacturing a slitted rotor is straightforward and needs only an appropriate lathe and a milling machine with a circular saw, e.g. according to DIN 138 diameter and thicknesses to manufacture e.g. 3 mm wide deep slits. However, a clearly higher performance can be achieved if a copper squirrel cage can be manufactured in a solid rotor core. If round copper bars are used, a cannon drill is needed as extra equipment. Drilled holes are needed to place round rotor bars in the construction. After drilling the holes the rotor can also be slitted. Open rotor slots are a benefit also in this case at least from the electromagnetic properties point of view [3]. Slitted surface, however, increases rotor surface friction. The slit under the round copper bar can offer a place for extra copper and a cooling channel. In addition, the slits work similarly as in a solid slitted rotor without squirrel cage making the main flux penetrate deeper into the rotor. Because the copper cage reduces the rotor resistance the rotor slip remains smaller than in a cageless rotor. Therefore, the flux also penetrates even better in the construction and a higher power factor of the system results [3]. Instead of round copper bars it is also possible to use other shapes that can be milled in the solid core and still have a mechanical locking feature. Slitting and slotting a solid rotor core, however, somewhat weakens its mechanical construction and, especially, slitting cannot necessarily be done as deep as would be favourable from the electromagnetic point of view but mechanical strength must be taken into account.

In case of a squirrel cage (Figure 1) there is a need to provide also short-circuit rings at the ends of the rotor active part. Mechanically these end rings are the most vulnerable parts of the rotor. Using for example CuCrZr material enables the strongest possible copper end ring but it does not usually survive in the rotor without some supporting construction. [4] The construction must enable the rotor cage thermal expansion. Therefore, the end rings should have some space to move axially during rotor heating and cooling. Because

J. Narsakka (corresponding author), T. Choudhury, and Prof. J. Sopanen are with Department of Mechanical Engineering, Lappeenranta-Lahti University of Technology LUT, Yliopistonkatu 34, 53850 Lappeenranta, Finland, Juuso.Narsakka@lut.fi & Tuhin.Choudhury@lut.fi & Jussi.Sopanen@lut.fi

Prof. E. Kurvinen is with Materials and Mechanical Engineering University of Oulu, Pentti Kaiteran katu 1, 90570 Oulu, Finland, Emil.Kurvinen@oulu.fi

K. Vostrov and Prof. J. Pyrhönen are with Department of Electrical Engineering, Lappeenranta-Lahti University of Technology LUT, Yliopistonkatu 34, 53850 Lappeenranta, Finland, Konstantin.Vostrov@lut.fi & Juha.Pyrhonen@lut.fi

of these reasons the design of a squirrel cage solid rotor is a challenging task that largely determines the motor mechanical and electromagnetic performance.

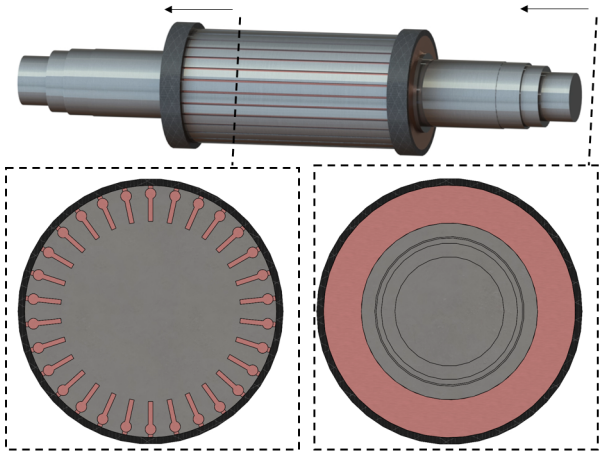

Fig. 1. Sketch of squirrel cage slitted solid rotor. On the left is the section view of the active part and on the right is the view from the end of the rotor.

Despite the importance of the mechanical construction, the design still must start with the electrical machine torque production evaluation, i.e. requirements for the design. [5] In the first hand it can be based on machine constant or Maxwell stress approach. Both approaches need assessment of the rotor type and the cooling method and cooling effectiveness. Typically, a well designed motor also has a favourable rotor length-to-diameter ratio. [3]. It can be used to evaluate different rotor topologies. After the preliminary topology is found mechanical and electrical design constrains have to be fit together. For that purpose this study aims to create a method for calculating a mechanically optimal structure using parameters related to electrical performance.

II. Analytical Methods for Conceptual Design of Slitted Squirrel Cage Rotor

The methods presented in this work are developed for rapid conceptual design for an electric machine's squirrel cage and slitted solid rotor for high-speed applications. A rapid design method enables easy analysis of the sensitivity of design changes for identifying the most optimal combinations of parameters. Mechanical design of the squirrel cage slitted rotor includes:

1. Slitted solid section possibly equipped with conductor bars
2. End ring design
3. Length of the active part
4. Design validation.

A. Slitted solid section with conductors bars

Rotor baseline creation for a slitted solid rotor type has been presented earlier, for example, by Kurvinen et al. [6]. In their study the focus was in presenting a step by step baseline calculation for a whole rotor supported by AMBs. In this study, the focus is adding a squirrel cage in a slitted solid rotor. A slitted solid rotor is not necessarily providing high enough torque per rotor volume and therefore the rotor conductivity must be increased. A squirrel cage made from copper bars and copper end rings offers a highly improved conduction capability for the rotor. In practice, the conductivity of copper at the operating temperature is more than tenfold compared to the conductivity of S355. In copper, the current density also is much more evenly distributed than in ferromagnetic steel conductors. Therefore, a solid rotor equipped with a squirrel cage enables significantly higher torque production with a better power factor than a slitted solid rotor. [7].

For electromagnetic design it is crucial to know the mechanical boundaries of the rotor structure. The number and cross section area of the bars, bars' distance from the surface and opening area of the slots are parameters which affect the electrical performance of the machine [7], [8]. For mechanical calculations those electrically important parameters can be used as inputs for baseline calculations. By varying those parameters a mechanical design space can be built for electrical design. Input parameters used in the baseline creation are presented in Table I and illustrated in Figure 2.

Rotor's active part mechanical design can be divided into two section: Bars in slitted solid rotor and design of end rings. Solid section design can be executed in the same way as presented in [2] by adding the bars in the calculation. An important stress location for the design can be found in the tooth root (w_{tooth}). Angular velocity causes a centrifugal force to pull the teeth and bars out from the solid rotor. The main steps of calculation are presented below. The maximum mechanical stress (σ_{tooth}) on a tooth root can be calculated as:

$$\sigma_{\text{tooth}} = \frac{(\rho_{\text{core}} A_{\text{tooth}} + \rho_{\text{bar}} A_{\text{bar}}) r_{\text{com}} \Omega^2}{w_{\text{tooth}}} k_{\text{tooth}} \qquad (1)$$

where ρ_{core} and ρ_{bar} are the density of rotor core and conductor material, A_{tooth} is the area of teeth, A_{bar} is the cross-sectional area of the conductor bar, r_{com} is the distance of teeth and bar mass centers from the axis of rotation. Ω is the angular velocity. w_{tooth} is the width of the tooth root. Stress concentration can be included by a multiplier factor k_{tooth} which can be analysed with FEM or obtained from predefined tables [9] and previous studies for similar structures [2]. Stress concentration factor is highly dependent on the radius of tooth side and its bottom. The dimensions of the saw determine usable nose radius of the cutting edge. For example, with 0.3 mm nose radius, 2.5 mm slits can be manufactured [2].

A_{tooth}, A_{bar} and r_{com} can be solved in relation of conductor bar radius (r_{b}) and its depth (h_{b}), slit width (w_{s}) and slit height (h_{s}). A cross-sectional view of teeth and bars is

presented in figure 2. A_{tooth} can be written then as:

$$A_{\text{tooth}} = \frac{(\pi(r_{\text{out}}^2 - (r_{\text{out}} - h_{\text{s}})^2) - w_{\text{s}} h_{\text{s}} n_{\text{s}}}{n_{\text{s}}} - 2r_{\text{b}}^2\left(\frac{\alpha}{2\pi} - \frac{1}{2}\sin\alpha\right) \tag{2}$$

where r_{out} is outer radius of active part and n_{s} is slit/bar number. α can be written as:

$$\alpha = 2\arccos\frac{w_{\text{s}}}{2r_{\text{b}}} \tag{3}$$

With case of round bar added rectangle shape below it A_{bar} can be simplified as:

$$A_{\text{bar}} = \pi r_{\text{b}}^2 + w_{\text{s}} h_{\text{rec}} \tag{4}$$

Where h_{rec} is rectangle height. For r_{com} calculation, center of teeth mass is predigested to be slit height divided by two. With usage of full cross section of bars the total center of mass is assumed to be slightly on the safe side (further from the rotational axis) from the exact value. r_{com} can be written as:

$$r_{\text{com}} = r_{\text{out}} - \frac{\frac{h_{\text{s}}}{2} A_{\text{tooth}}\rho_{\text{core}} + (\pi r_{\text{b}}^2(h_{\text{b}} + r_{\text{b}}) + w_{\text{s}} h_{\text{s}}(h_{\text{b}} + 2r_{\text{b}} + \frac{h_{\text{rec}}}{2}))\rho_{\text{bar}}}{A_{\text{tooth}}\rho_{\text{core}} + A_{\text{bar}}\rho_{\text{bar}}} \tag{5}$$

Now by substituting the equations 2, 3, 4 and 5 into equation 1 the maximum value of rotor radius can be iterated with electrical input parameters and e.g., different material strengths.

Electromagnetic constraints must be taken into account in all cases. One important thing is to maintain large enough magnetic flux paths during the rotor mechanical design. There are two narrow points i.e. between rotor bars round section (w_{tooth2}) and in the tooth root (w_{tooth}), see Fig. 2. The fundamental air-gap peak flux density in electrical machines typically is close to 1 T. Saturation polarization of steel is typically slightly over 2 T. Based on this, the teeth must be wide enough not to saturate. Therefore, the iron width between rotor copper bars and between teeth bottoms must not be less than about 50% of the rotor slot pitch on the air gap surface. [3]. This can be kept as a starting point that can later be refined in the electromagnetic design of the machine.

This method for determining rotor active part dimensions can be used without bar area to calculate parameters for a slitted rotor type as well. The method is also easily adaptable for other basic geometric shapes e.g., trapezoidal bar model.

B. End ring design

Electrical requirements for the end ring design come from the cross-sectional surface area of rotor bars. In a two-pole induction machine, half of the rotor bars carry current into same direction at the same time. The current density in different bars is following a sinusoidal patter. The ring current

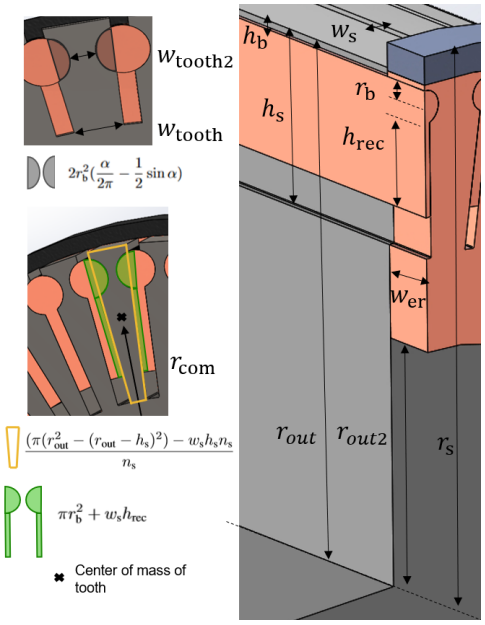

Fig. 2. Sections for slit tooth root and end ring stress calculation.

is therefore accumulating from rotor bars, covering a half of the two-pole rotor. Accumulated current in the end ring can be calculated by following Kirchhoff's first law at each of bar connection points. [3]. Because the induced current frequency (slip frequency) is low, current can be assumed equally distributed in the end ring and thus bars area can be compared to the end ring cross section area. The end ring outer radius can at maximum equal the outer radius of the active part and the minimum radius is dictated by the rotor shaft diameter (r_{out2}). The axial length of the end ring (w_{er}) can be thus calculated as:

$$w_{\text{er}} = \frac{A_{\text{bar}}}{2\sin\frac{2\pi p_{\text{n}}}{2n_{\text{s}}}(r_{\text{out}} - r_{\text{out2}})} \tag{6}$$

Where p_{n} is number of pole pairs in electric machine. According to Eq. 6 the end ring should be made of as conductive material as the rotor conductor bars. Highly conductive materials like copper are not as strong as materials usable in the rotor core. A sleeve over the end ring can be used to reduce the stresses in the end ring. The sleeve should preferably be made of non-magnetic material to minimize the end ring leakage flux. [7] Other difficulty lies in attachment between the bars and the end rings. From a conceptual design point of view too detailed construction is not reasonable. The solution presented here is based on an idea to get the radial displacement of the rotor active part and the end ring on the same level at the rated speed. With this idea the end ring and the bar attachment stresses can be kept in low level. To implement the idea, equations for a tubular cylinder under pressure loading can be applied. Outer radius of a sleeve (r_{s}) can be calculated from the stress of a cylindrical ring under pressure (Eq. 10) when the rated speed displacement difference of the active part and the end ring are known (Eq. 7, 8). The displacement difference can be used to calculate

the required pressure against the end ring outer surface to generate the same displacement but in opposite direction (Eq. 9). Displacements can be estimated from equations for a disc under angular velocity as: [10].

$$\Delta r_{\text{ac}} = \frac{\rho_{\text{core}}\Omega^2 r_{\text{out}}}{4E_{\text{core}}}[(1-\nu_{\text{core}})r_{\text{out}}^2] \tag{7}$$

where Δr_{ac}, E_{core}, ν_{core} are the radial displacement of the rotor active part, the rotor core material modulus of elasticity and Poisson's ratio, respectively. It should be noted that Eq. 7 does not take into account the slits and bars and it is intended to be used with disc type structures. Thus, the equation is more suitable to calculate the end ring displacement which can be written as:

$$\Delta r_{\text{er}} = \frac{\rho_{\text{er}}\Omega^2 r_{\text{out}}}{4E_{\text{er}}}[(1-\nu_{\text{er}})r_{\text{out}}^2 + (3+\nu_{\text{er}})r_{\text{out2}}^2] \tag{8}$$

where Δr_{er}, ρ_{er}, E_{er}, ν_{er} are the end ring displacement, density, modulus of elasticity (with anisotropic materials circumferential) and Poisson's ratio. Now the displacement difference of the end ring and the active part (δ) can be used to solve the required pre-pressure for the end ring outer surface from equation 9. [10]

$$\delta = \frac{1}{E_{\text{er}}(r_{\text{out}}^2 - r_{\text{out2}}^2)}[(1-\nu_{\text{er}}) - pr_{\text{out}}^3 + (1+\nu_{\text{er}})r_{\text{out}}r_{\text{out2}}^2(-p)] \tag{9}$$

By substituting the maximum stress of the sleeve (σ_{smax}) and p to Eq. 10 the outer diameter of the sleeve can be solved [10]. If the pre-pressure is on a high level it can be e.g., divided by two to half the effect. It is also good to check the sleeve displacement due to angular velocity with equation 8 (with sleeve parameters) to know if the attachment pressure between the end ring and the sleeve increases or decreases as a result of velocity.

$$\sigma_{\text{smax}} = \frac{r_{\text{s}}^2 + r_{\text{out}}^2}{r_{\text{s}}^2 - r_{\text{out}}^2}p \tag{10}$$

Radial thermal expansion can be taken into account by using thermal expansion coefficient difference between the end ring and the rotor core [11]. The displacement difference (Δr_{tem}) can be then written as:

$$\Delta r_{\text{tem}} = (\alpha_{\text{er}} - \alpha_{\text{ac}})r_{\text{out}}\Delta T \tag{11}$$

Where α_{er} and α_{ac} are the thermal expansion coefficients of the end ring and the active part. ΔT is the temperature difference between operating and room temperature. Δr_{tem} can be added to δ when temperature difference is considered in calculations.

C. Length of the active part

When the maximum radius of the active part, the end ring, and the sleeve have been calculated, the length of the active part (l_{ac}) can be calculated from the mechanical machine constant (C_{mec}). The constant is based on information of well-designed similar electrical machines. In [3] is presented a figure of mechanical power of asynchronous and synchronous machines in relation of mechanical machine constant. With curve fitting method it can be obtained equations (13,14) for C_{mec} average value which can be used to calculate the length of the active part as:

$$l_{\text{ac}} = \frac{P}{C_{\text{mec}}(2r_{\text{out}})^2\frac{\Omega}{2\pi p_{\text{n}}}} \tag{12}$$

$$C_{\text{mec2-6}} = 110.8(\frac{P}{2p_{\text{n}}})^{0.1667} \tag{13}$$

$$C_{\text{mec1}} = 73.62(\frac{P}{2p_{\text{n}}})^{0.1588} \tag{14}$$

$C_{\text{mec2-6}}$ is mechanical machine constant for 2 - 6 pole pair machines and C_{mec1} is for one pole pair machines. When comparing squirrel cage configurations the machine constant does not offer the difference. For more detailed analysis of mechanical and electromagnetic properties, FEM must be used. [3]

D. Validation of the analytical method

The suitability of presented method can be evaluated with finite element analysis. There are four main areas of interest:
1. Suitability of the analytical method for tooth stress with conductor bars.
2. Stress concentration factor in tooth.
3. Suitability of the disc strain equation with slitted disc type structure.
4. Suitability of the analytical calculation for sleeve structure.

III. Testing the presented design method with cases from literature

Three cases from literature are selected for testing the presented design method. The first case is a solid rotor with a squirrel cage rotor (round bars with the slot opening) for ultra high-speed (120 000 rpm) in 6 kW range, presented in [7]. The second case is a laminated squirrel cage rotor for 21 kW and 50 000 rpm [12]. The third case is a slitted solid rotor in megawatt range (2 MW) with rotational speed of 12 000 rpm, presented in. [13]. Initial requirements and design results for the cases are presented in Table I and Table II respectively. The results were iterated with purpose to design maximum radius with maximum depth of the slits (bars). In the calculations, bar rectangular shape was set to be 0.8 · height of the slit. As end ring sleeve material, Titanium was used.

Any of the literature cases did not match exactly with the presented keyhole (round + rectangular) bar design. For literature case 3 three different designs were created to test the method more widely. S700 steel was selected for the rotor core material and copper-based metal matrix composite (Glidcop®) with 460 MPa yield strength was selected for the conductor bars. Carbon-fibre composite was used for sleeve material. Power, speed, pole number, slit width, bar diameter, and minimum end ring inner diameter were kept as presented in Table I. The target for

TABLE I
BASELINE DIMENSIONS FROM LITERATURE CASES

Parameters	Case 1 [7]	Case 2 [12]	Case 3 [13]
Input values			
Speed (rpm)	120 000	50 000	12 000
Power (kW)	6	21	2 000
Number of pole pairs	1	1	1
Number of bars	18	17	44
Bar diameter (mm)*	3	5	12**
Slit width (mm)*	0.5	2**	4
End ring radius in (mm)*	9.2	15	87.5**

* Measured from figures presented in reference case design
** Not included in case design from literature

TABLE II
BASELINE DIMENSIONS VERSUS LITERATURE CASES

	Ref.	Baseline	Deviation (%)
Case 1			
Rotor diameter (mm)	30.7	29	-5.5
Surface velocity (m/s)	193	182	-5.5
Slit depth (mm)	-	7.7	-
Active length (mm)	50	40.7	-18.6
Sleeve thickness (mm)*	1	1.2	20.0
C_{mec1} (kWs/m^3)	66.7	87.7	31.5
Max. stress on rotor core	567	760**	-
Nominal stress on tooth	-	190	-
Max. stress on end ring	258	140	-45.7
Max. stress on end ring (no sleeve)	-	259	-
Max. stress on sleeve	667	input 667	-
Case 2			
Rotor diameter (mm)	51	57.8	13.3
Surface velocity (m/s)	133	151	13.3
Slit depth (mm)	-	17.8	-
Active length (mm)	102	70.5	-30.9
Sleeve thickness (mm)	-	1.5	-
C_{mec1} (kWs/m^3)	95***	107	12.6
Max. stress on rotor core	-	600**	-
Nominal stress on tooth	-	150	-
Max. stress on end ring	-	110	-
Max. stress on end ring (no sleeve)	-	230	-
Max. stress on sleeve	-	input 667	-
Case 3			
Rotor diameter (mm)	266	226	-15.0
Surface velocity (m/s)	167	141	-15.0
Slit depth (mm)	50	41.9	-16.2
Active length (mm)	538	888	65.1
Sleeve thickness (mm)	-	10.3	-
C_{mec1} (kWs/m^3)	263***	220	-16.3
Max. stress on rotor core	-	355**	-
Nominal stress on tooth	-	89	-
Max. stress on end ring	-	20	-
Max. stress on end ring (no sleeve)	-	168	-
Max. stress on sleeve	-	input 667	-

Deviation = abs(Ref-Baseline) / Ref · 100
* Measured from figures presented in reference case design
** Max. stress used in case design from literature
*** Calculated value from literature case

the design iteration was to reach the maximum total bar cross sectional area. Design iteration includes only a bar number variation from 10 to 80 bars. With round bars 12 mm and 20 mm diameters were used. With 20 mm bar diameter higher total cross sectional area of bars was reached. The results of the designs are presented in Table III.

Analytically calculated results were validated with FE-analysis. The keyhole design with 0.7 · slit depth bar height was selected for comparison (0.3 was wanted to kept for cooling, which will be studied in future). The results are presented in Table IV. The minus in the table means compressive stress and case of displacement, movement in radial direction closer to the axis.

TABLE III
PROPOSED DESIGN METHOD USED WITH LITERATURE CASE 3. FOR THE ROTOR CORE, TENSILE STRENGTH IS SET TO 700 MPA AND FOR THE CONDUCTOR MATERIAL 460 MPA, FOR SLEEVE ELASTIC MODULUS IS USED 120 GPA

Parameter	**Round bar d 20 mm**	**keyhole d 12 mm + 0.7h_s**	**keyhole d 12 mm + 1h_s**
Bar number	21	40	40
Bars area (mm^2)	6597	9808	11866
Diameter (mm)	455	363	353
Surface velocity (m/s)	286	228	222
Slit depth (mm)	58.7	61.2	59.9
Tooth root width (mm)	46.6	15	14.4
End ring width (mm)	6	18	24
End ring height (mm)	140	94	89
End ring stress no s. (MPa)	626	405	384
Sleeve thickness (mm)	56	29	27
Sleeve stress (MPa)	667	667	667
End ring stress with s. (MPa)	287	147	135

TABLE IV
COMPARISON OF ANALYTICALLY CALCULATED VALUES WITH FE-ANALYSIS. CONFIGURATION USED IN COMPARISON IS RESULTS OF TABLE III KEYHOLE ($0.7h_s$) BAR CASE.

Parameters	**Analytical**	**FEM**
Tooth nominal stress (MPa)	175	172
Max. stress in tooth root (MPa)	-	740
Tooth stress concentration (MPa)	-	4.3
Displacements (mm)		
- In active part	0.06	0.1
- In end ring (without sleeve)	0.25	0.25
Attachment pressure (MPa)	99	-
Required sleeve thickness	29	-
Max. stress from attach. in e.r. (MPa)	-258	-257
Max. stress from attach. in s. (MPa)	667	720
Displacements from attachment	-0.19	- 0.20
Max. stress in rated speed e.r. (MPa)	147	139
Max. stress in rated speed s. (MPa)	667	720
Displacement in rated speed (mm)	0.06	0.065

To get on insight for the electromagnetic performance of squirrel cage slitted solid rotor FEM analyses were performed for four different rotor cross sections. Fig. 3 show the geometries being modelled and torque capacities in relation of per-unit slip. Literature case 3 was analyzed as 'Case 0'. 'Case 1' is modified 'literature case 3' rotor configuration, where slits are replaced with 12 mm round bars. 'Case 2' is the combination of slitted rotor and squirrel-cage with round bars. Rotor with extra rectangular bars filling half of the slits is modelled as 'Case 3'.

IV. DISCUSSION

The purpose of the work was to develop an analytical method to analyze and match stresses in a squirrel cage slitted solid rotor. With open rotor slots a wider range of manufacturing methods can be used and thus different conductor bar configurations are available. In active part,

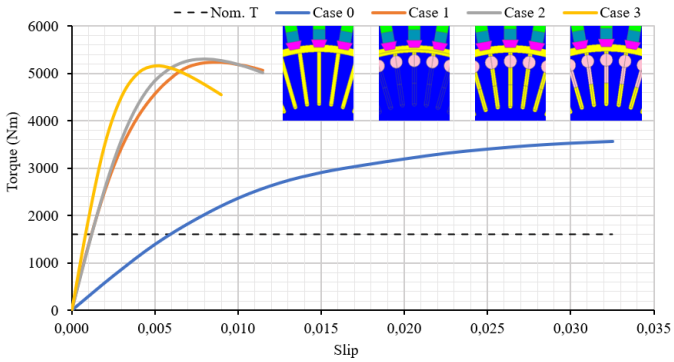

Fig. 3. Torque capacity in relation to the per-unit slip for four different rotor types based on the literature case 3 (see table I). The bar diameter is 12 mm, the slit width is 4 mm, and the slit depth from the rotor surface is 50 mm. The rated speed slip for the case 3 is 0,0008 and the case 1 & 2 0,0012

tooth stresses calculated from centrifugal force with stress concentration factor resulted in high accuracy. With the analytical method, thousands of designs can be calculated in seconds while with FEA, one configuration can take several minutes. The restriction from electrical viewpoint to keep the total width of teeth roots and bar gaps in a minimum of half of the circumference turned out to be good from the mechanical aspect as well. With that restriction, mechanical stresses between the bars stay at the minimum in the same level as tooth root.

The method for end ring design was quite accurate and efficient as well. The only larger deviation between analytical and FEA results was in the active part radial displacement. That is probably due to higher tooth strain than in a solid disc which was used to calculate the displacement. The rotor displacement equation can be updated to contain solid and tooth sections separately to reach more accurate results. Calculated by the current displacement, the sleeve will be too tight, resulting in unnecessary sleeve thickness. The downside of the sleeve design can be found from the difficulty to design its outer surface at the same level than the active part. Using a thick sleeve it can interfere with cooling flow on the rotor surface. If the cooling can be arranged to work with the sleeve, it offers a high reduction of stresses in critical end ring and bar attachment locations. The method proposed in this study does not account for ways to attach the bars with the rings. Different methods have been studied [7], [8], [14] in the past but one solution for general use has not been proposed. Future studies should include analysis on how different operation speeds affect the difference in displacement, and thus fluctuating stresses which could lead to a fatigue failure. Also, manufacturing tolerances are needed to be studied to evaluate attachment pressure error margin. The results make it possible to better define how the attachment between the end ring and the bars should be implemented.

The presented keyhole design was compared with literature cases where slightly different squirrel cage rotor configuration was designed up to manufacturing level. In cases 1 and 2 machines were also experimentally tested to verify the designs. In case 1, keyhole design has 5.5 % smaller diameter, but it contains additional conductor bar cross section under the round bar. In case 2, literature rotor is constructed with a solid shaft and lamination. Laminated rotors contain higher stresses and lower natural frequencies and thus do not exceed as high diameter in active part as keyhole design. In case 3, the literature rotor is not equipped with conductor bars and thus it reaches a higher diameter. Mechanical machine constants vary a bit and it could be investigated more precisely by power category. However, it is usable for calculation of the rotor length which is utilized whole rotor baseline model creation [6] to study preliminary dynamic behavior of rotor. Deviation in end ring stresses in case 1 is probably due to stresses caused by attachment of end ring and bars. In this study sleeve for end ring was designed to be attached at a pre-stress level which minimizes strain between bar and end ring at operation speed. Due to that high stress did not emerge. Stresses and especially stress concentrations are highly dependent on attachment type which was not studied in this paper.

Preliminary rotor design was executed in the study for a 2 MW 12 000 rpm machine. Keyhole design was observed to be better than the round bar design due to decreased slip of the rotor. The potential effect of slit cooling was not analyzed in this work, but will be investigated in the future. Active part diameters resulted in much higher radius than in a compared literature case. Which suggests that an attempt could also be made to design a partially [12] or fully laminated rotor type for the case diameter. In the literature can be found that over 200 m/s surface velocities for squirrel-cage solid rotor designs [8], [15], [16] are typical values, which confirm the calculations. The main reason for the larger diameter can be found from higher material strength of rotor core material. From the results can be also seen that bars do not increase considerably the tooth root stress. Taking into account the results of figure 3, it can be easily said that bars should be included in the design without exception. That will even more underline the importance of continuation of end ring design study.

The most important result of the study was the understanding of the importance of a right design procedure. Especially, in situations when designing an electric machine out of the well-known area mechanical design exploration is crucial for an efficient design process. With the design exploration electrical designers can easily find mechanical limitations for different configurations. That makes it more straightforward to analyse accurate tangential stress values to determine rotor length which can be used in machine dynamic analysis. It will also help the manufacturing experts to participate the process from the beginning of the design.

V. CONCLUSIONS

The work presented an analytical calculation method that can be used to calculate the mechanical limit values for a squirrel cage solid slitted rotor model when high rotational speed is the restrictive factor. The method can be used with various bar types but presented equations are limited for keyhole bar configuration. The research cases in prototype level selected from the literature showed the ability, efficiency and validity of the calculation method. The method can be further integrate into the entire rotor design process.

REFERENCES

[1] J. Pyrhönen, J. Nerg, A. Mikkola, J. Sopanen, and T. Aho, "Electromagnetic and mechanical design aspects of a high-speed solid-rotor induction machine with no separate copper electric circuit in the megawatt range," *Electrical engineering*, vol. 91, no. 1, pp. 35–49, 2009.

[2] T. Aho, J. Nerg, J. Sopanen, J. Huppunen, and J. Pyrhönen, "Analyzing the effect of the rotor slit depth on the electric and mechanical performance of a solid-rotor induction motor," *International Review of Electrical Engineering (IREE)*, vol. 1, no. 4, pp. 516–525, 2006.

[3] J. Pyrhönen, *Design of rotating electrical machines*, 2nd ed. Chichester: Wiley, 2014.

[4] D. Gerada, A. Mebarki, N. L. Brown, C. Gerada, A. Cavagnino, and A. Boglietti, "High-speed electrical machines: Technologies, trends, and developments," *IEEE Transactions on Industrial Electronics*, vol. 61, no. 6, pp. 2946–2959, 2014.

[5] E. Kurvinen, C. Di, I. Petrov, J. Nerg, O. Liukkonen, R. P. Jastrzebski, D. Kepsu, P. Jaatinen, L. Aarniovuori, E. Sikanen *et al.*, "Design and manufacturing of a modular low-voltage multimegawatt high-speed solid-rotor induction motor," *IEEE Transactions on Industry Applications*, vol. 57, no. 6, pp. 6903–6912, 2021.

[6] E. Kurvinen, T. Choudhury, J. Narsakka, I. Martikainen, J. Sopanen, and R. P. Jastrzebski, "Design space method for conceptual design exploration of high speed slitted solid induction motor," in *2021 IEEE International Electric Machines & Drives Conference (IEMDC)*. IEEE, 2021, pp. 1–8.

[7] J. Barta, N. Uzhegov, P. Losak, C. Ondrusek, M. Mach, and J. Pyrhönen, "Squirrel-cage rotor design and manufacturing for high-speed applications," *IEEE Transactions on Industrial Electronics*, vol. 66, no. 9, pp. 6768–6778, 2018.

[8] T. Mauffrey, J.-F. Pradurat, L. Durantay, and J. Fontini, "Comparison of 5 different squirrel cage rotor designs for large high speed induction motors," in *PCIC Europe 2013*. IEEE, 2013, pp. 1–9.

[9] W. D. Pilkey, D. F. Pilkey, and Z. Bi, *Peterson's stress concentration factors*. John Wiley & Sons, 2020.

[10] R. G. Budynas and J. K. Nisbett, *Shigley's mechanical engineering design. 9th ed.* New York: McGraw-Hill., 2011.

[11] N. Uzhegov, E. Kurvinen, J. Nerg, J. Pyrhönen, J. T. Sopanen, and S. Shirinskii, "Multidisciplinary design process of a 6-slot 2-pole high-speed permanent-magnet synchronous machine," *IEEE Transactions on Industrial Electronics*, vol. 63, no. 2, pp. 784–795, 2015.

[12] W. L. Soong, G. B. Kliman, R. N. Johnson, R. A. White, and J. E. Miller, "Novel high-speed induction motor for a commercial centrifugal compressor," *IEEE Transactions on Industry Applications*, vol. 36, no. 3, pp. 706–713, 2000.

[13] C. Di, "Modeling and analysis of a high-speed solid-rotor induction machine," Ph.D. dissertation, Lappeenranta-Lahti University of Technology, 2020.

[14] M. A. Kabir, R. Mikail, S. Englebretson, and I. Husain, "3d fea based squirrel cage rotor model for design tradeoffs and performance analysis," in *2015 IEEE Applied Power Electronics Conference and Exposition (APEC)*. IEEE, 2015, pp. 2696–2702.

[15] R. Lateb, J. Enon, and L. Durantay, "High speed, high power electrical induction motor technologies for integrated compressors," in *2009 International Conference on Electrical Machines and Systems*. IEEE, 2009, pp. 1–5.

[16] D. Gerada, A. Mebarki, N. L. Brown, K. J. Bradley, and C. Gerada, "Design aspects of high-speed high-power-density laminated-rotor induction machines," *IEEE Transactions on Industrial Electronics*, vol. 58, no. 9, pp. 4039–4047, 2010.

VI. BIOGRAPHIES

Juuso Narsakka was born in Rautjärvi, Finland, in 1989. He received M. Sc. (Tech.) degrees in mechanical engineering from Lappeenranta University of Technology (LUT) in 2022, where he is currently pursuing the D. Sc. (Tech.) degrees in mechanical engineering. His research interests are in the design of high-speed rotating machines where is needed combination of an understanding of machine dynamics and strength of materials. His work history includes jobs in industry, entrepreneurship, and teaching in LUT University.

Konstantin Vostrov was born in Leningrad, Russia, in 1991. He received the B.Sc. degree in the field of Electrical Engineering, Electromechanics and Electrotechnology from Peter the Great St. Petersburg Polytechnic University in 2013, and the double-degree M.Sc from the Peter the Great St. Petersburg Polytechnic University and Lappeenranta University of Technology in 2016. He is currently a doctoral student at Lappeenranta University of Technology. His research interests are in the field of electrical engineering and include electrical machines and electrical drives.

Tuhin Choudhury was born in Seppa, India, in 1989. He received the B.Sc. (tech) degree in mechanical engineering from Sikkim Manipal University, India, in 2011, and the M.Sc. degree in mechatronic system design from LUT University, Lappeenranta, Finland, in 2018, where he is currently pursuing the Ph.D. degree with the Department of Mechanical Engineering. He was a design engineer on the development of medical devices and diagnostic instruments, from 2011 to 2016. His research interests include designing, modeling, and simulation of rotating machines, and the analysis of rotor behavior to understand the root cause of unwanted vibrations, specifically due to unbalance.

Emil Kurvinen was born in 1988. He received M. Sc. (Tech.) and D. Sc. (Tech.) degrees in mechanical engineering from Lappeenranta University of Technology (LUT) in 2012 and 2016, respectively. In 2014-2015 he visited University of Virginia as a Fulbright visiting scholar researching active magnetic bearings. In 2016 to 2017 he served as a engineer, structural dynamics in FS Dynamics Finland Ltd. In 2017-2021 he was as a postdoctoral researcher at LUT. Currently he is Machine Design professor in University of Oulu. He has a solid background in machine design, especially in the design, simulation, analysing of rotating machines. His research interests are rotating machines, especially high-speed machines, digital twins and integration of industrial engineering and management to technology.

Jussi Sopanen (Member, IEEE) was born in Enonkoski, Finland, in 1974. He received the M.Sc. degree in mechanical engineering and the D.Sc. (technology) degree from LUT University, Lappeenranta, Finland, in 1999 and 2004, respectively. He was a Researcher with the Department of Mechanical Engineering, LUT University, from 1999 to 2006. He was a Product Development Engineer of electric machine manufacturing with Rotatek Finland Ltd. from 2004 to 2005. From 2006 to 2012, he was a Principal Lecturer in mechanical engineering and the Research Manager of the Faculty of Technology, Saimaa University of Applied Sciences, Lappeenranta. He is currently serving as a Professor with the Machine Dynamics Laboratory, LUT University. His research interests include rotor dynamics, multibody dynamics, and the mechanical design of electrical machines.

Juha Pyrhönen (Senior Member, IEEE) was born in Kuusankoski, Finland, in 1957. He received the D.Sc. degree in electrical engineering from the Lappeenranta University of Technology (LUT), Lappeenranta, Finland, in 1991.,He became a Professor of Electrical Machines and Drives in 1997 with LUT. He is engaged in research and development of electric motors and power-electronic-controlled drives. His research interests include development of special electric drives for distributed power production, traction, and high-speed applications, and permanent magnet materials and applying them in machines. He is currently researching new carbon-based materials for electrical machines.